

Intrazeolite Photochemistry. 11. Modification of the Properties of the Energy-Transfer Photosensitizer 4-Aminobenzophenone by Immobilization within Different Zeolite Microenvironments

María V. Baldoví,[†] Frances L. Cozens,[‡] Vicente Fornés,[†]
Hermenegildo García,^{*,†} and J. C. Scaiano^{*,‡}

*Instituto de Tecnología Química CSIC-UPV, Universidad Politécnica de Valencia,
46071 Valencia, Spain, and Department of Chemistry, University of Ottawa,
Ottawa, Canada, K1N 6N5*

Received July 10, 1995. Revised Manuscript Received September 25, 1995[§]

4-Aminobenzophenone (ABP) has been incorporated within the internal voids of four acid zeolites (HY, H β , HMor, and HZSM5) and the resulting composites characterized by diffuse reflectance, thermogravimetric analysis–differential scanning calorimetry, and FT-IR. Time-resolved diffuse reflectance of these composites showed that the photochemistry of ABP within these solids after laser excitation is extremely dependent on the zeolite microenvironment. The transient reflectance spectrum obtained for the ABP–HY composite closely resembles the transient absorption spectrum for ABP in polar solvents. However, the transient reflectance spectrum obtained for the ABP–HZSM5 composite shows one maximum at 530 nm, due to the T–T absorption of ABPH⁺ triplet. A different situation was found for the ABP–H β and ABP–HMor composites, where besides the reflectance at 530 nm, other bands were present. In addition, the zeolite framework also modifies how ABP behaves as a photosensitizer. The use of these composites as heterogeneous photosensitizers was explored by performing the photosensitized dimerization of 1,3-cyclohexadiene as a model reaction. Cyclobutane [2+2] dimers were the main products, indicating that an energy-transfer reaction is the predominant mechanism under these conditions.

Introduction

Photochemistry of organic compounds in organized and constrained media is a topic of current interest.¹ Among the different hosts, zeolites are considered to be one of the most versatile.^{2,3} This is mainly due to the fact that these crystalline aluminosilicates, while exhibiting a high degree of thermal, chemical, and photochemical stability, can be obtained in a wide variety of chemical compositions and crystalline structures.⁴ Thus, an array of well-defined chemical and topological environments are available to accommodate the desired transformation of the guest molecule.⁵

The use of zeolites in organic photochemistry has been almost exclusively limited to the direct photolysis of an incorporated guest. A large number of examples have been reported showing the remarkable influence of the size, shape, and chemical composition of the zeolite on the course of the photochemical reaction.⁶ However, no systematic application using zeolites as hosts for sensitized photochemical reactions has been reported. This

is despite the fact that a tool to gain control on photosensitized transformations would be highly desirable. Among the rather rare examples of sensitization by zeolite guests are recent reports by Frei^{7–9} of zeolite-assisted olefin photooxidation, and energy- and electron-transfer processes involving aromatic and heteroaromatic cations.^{10–13}

Heterogeneous systems displaying shape selectivity can be designed by confinement of the active site within a restricted space.¹⁴ In the case of thermal ground-state reactions, a large amount of information about the use of zeolites as shape-selective acid catalysts is available, and application to other types of reactions such as base catalysis, oxidation, and asymmetric synthesis is an active area of research.¹⁵ Generally, the active sites responsible for the catalysis are part of the zeolite framework or are chemically bonded to it.

Therefore, to develop zeolitic composite materials that can be used as heterogeneous photosensitizers in or-

[§] Abstract published in *Advance ACS Abstracts*, November 1, 1995.

(1) Ramamurthy, V. *Photochemistry in Organized and Constrained Media*; VCH: New York, 1991.

(2) Ramamurthy, V.; Eaton, D. F.; Caspar, J. V. *Acc. Chem. Res.* **1992**, *25*, 299.

(3) Gessner, F.; Scaiano, J. C. *J. Photochem. Photobiol. A: Chem.* **1992**, *67*, 91.

(4) *Introduction to Zeolite Science and Practice*; van Bekkum, H., Flanigen, E. M., Jansen, J. C., Eds.; Elsevier: Amsterdam, 1991.

(5) Smith, J. V. *Chem. Rev.* **1988**, *88*, 149.

(6) Ramamurthy, V. Photoprocesses of Organic Molecules Included in Zeolites. In *Photochemistry in Organized and Constrained Media*; Ramamurthy, V., Ed.; VCH: New York, 1991; Chapter 10.

(7) Blatter, F.; Frei, H. *J. Am. Chem. Soc.* **1994**, *116*, 1812.
(8) Blatter, F.; Moreau, F.; Frei, H. *J. Phys. Chem.* **1994**, *98*, 13403.
(9) Blatter, F.; Frei, H. *J. Am. Chem. Soc.* **1993**, *115*, 7501.
(10) Brigham, E. S.; Snowden, P. T.; Kim, Y., I.; Mallouk, T. E. *J. Phys. Chem.* **1993**, *97*, 8650.

(11) Corma, A.; Fornés, V.; García, H.; Miranda, M. A.; Primo, J.; Sabater, M. J. *J. Am. Chem. Soc.* **1994**, *116*, 2276.

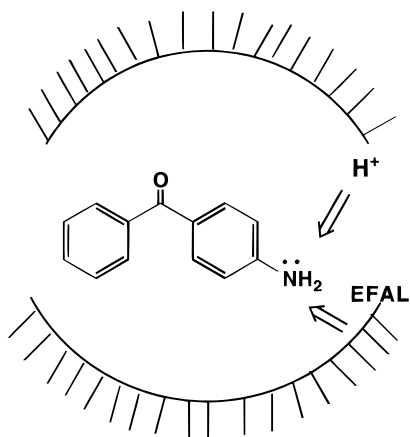
(12) Corma, A.; Fornés, V.; García, H.; Miranda, M. A.; Sabater, M. J. *J. Am. Chem. Soc.* **1994**, *116*, 9767.

(13) Baldoví, M. V.; Corma, A.; García, H.; Martí, V. *Tetrahedron Lett.* **1994**, *35*, 9447.

(14) Chen, N. Y.; Garwood, W. E.; Dwyer, F. G. *Shape Selective Catalysis in Industrial Applications*; Marcel Dekker: New York, 1989.

(15) Davis, M. E. *Acc. Chem. Res.* **1993**, *26*, 111.

Scheme 1. Immobilization of ABP within the Internal Surfaces of Zeolites by Interaction with Acid Sites (Both Bronsted (H^+) or Lewis (EFAL))



ganic reactions, it would be very convenient to immobilize the sensitizer molecules on the internal cavities of the solid host. This immobilization within a closed environment might impose geometrical restrictions and/or a polarity effect on the product distribution, depending on the size and chemical composition of the space where the reactions occur. Zeolites are particularly appropriate for this purpose as a consistent series of solids exhibiting distinctive shape, free volume, and chemical composition of the reaction cavity are easily available. These systems allow prior characterization of any modification caused on the sensitizer excited states by interactions with the zeolite framework. In addition, from a preparative point of view, the use of heterogeneous photosensitizers would have the advantage of easy workup and separation of the reaction mixture.

In the present work, we report on the preparation, characterization, and energy-transfer properties of a benzophenone derivative within different zeolites. We show that the nature of the excited states of the guest sensitizer as well as its interaction with quenchers are strongly dependent on the geometrical characteristics of the reaction cavity where the photosensitizer is located. In the present study we have chosen a substituted benzophenone as the guest sensitizer due to their frequent use as energy-transfer sensitizers.¹⁶ In particular, 4-aminobenzophenone (ABP) was the photosensitizer of choice since we reasoned that the moderate basicity introduced by the aromatic amino group would anchor this molecule onto the internal surface of acidic zeolites (Scheme 1). Recently, we have shown that the active sites of acid faujasites can intervene with the course of photochemical reactions, modifying the characteristic reactivity pattern of α,α -diphenyl-substituted acetones¹⁷ and assisting the photochemical azobenzene disproportionation.¹⁸ Herein, we report on another application of these materials.

To attain materials displaying a useful variety of sizes and shapes of internal voids, we have employed four different acidic zeolites. The framework structure varies from the large-pore tridirectional zeolites (Y) and

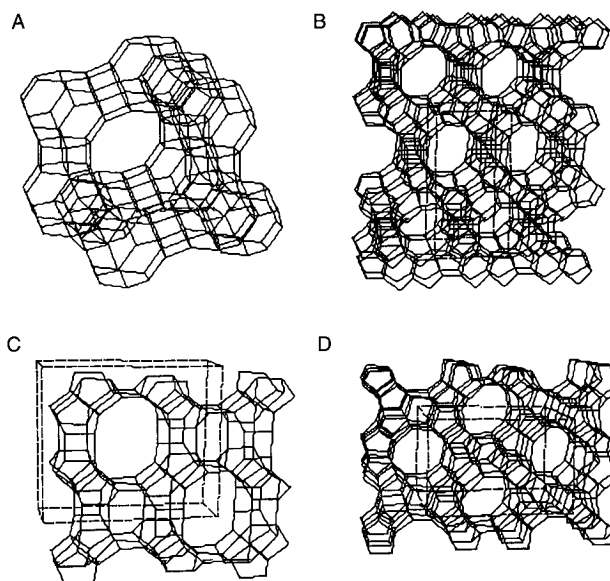


Figure 1. Visualization of the framework structures of (A) zeolite Y, (B) β , (C) mordenite, and (D) ZSM5.

bidirectional (β) and monodirectional zeolite (Mordenite) to the medium-pore (ZSM5) zeolite.¹⁹ A visualization of the framework structure of the zeolites used in this study are presented in Figure 1. The aim of this work is to determine how the microenvironment experienced by the guest influences its properties as a photosensitizer.

Experimental Section

Preparation of the Acidic Zeolites. HY was prepared by stirring a commercial NaY sample (Union Carbide SK40) with a 0.4 M aqueous solution of NH₄AcO using a solid–liquid weight ratio of 1:4 at 298 K for 30 min. The resulting solid was filtered, thoroughly washed with distilled water, dried at 383 K for 6 h, and finally deep-bed calcinated at 823 K for 3 h. The partially exchanged sample was submitted to an additional ion exchange–calcination treatment with a 0.6 M solution of NH₄AcO following the above experimental procedure. The unit-cell size measured according to ASTM D-3942-8 was 24.41 Å, while the crystallinity determined by X-ray diffraction (XRD) was 85%. H β zeolite was prepared starting from a synthetic β sample in its tetraethylammonium form by heating at 773 K under a stream of N₂ and calcination in the air at 823 K, followed by two NH₄⁺ exchange–calcination cycles.²⁰ HMor was prepared by heating a commercial sample in its sodium form (P. Q. Industries Si/Al 6) with 1 M hydrochloric acid at 343 K for 30 min.²¹ The solid was filtered, washed thoroughly with distilled water, and dried at 383 K for 6 h. HZSM5 zeolite was synthesized following the procedure reported in the literature.²² After calcination at 823 K to remove the organic material, it was twice exchanged with NH₄⁺ and baked at 823 K for 3 h.

The crystal sizes of the zeolites were determined by scanning electron microscopy. BET surface areas were measured by N₂ adsorption and desorption (Table 1). Acidity of the zeolites by pyridine adsorption was measured with a Perkin-Elmer 580 B FT-IR spectrophotometer equipped with a data station according to the reported procedure.²³

(19) Meier, W. M.; Olson, D. H. *Atlas of Zeolite Structure Types*; Butterworth: London, 1992.

(20) Pérez-Pariente, J.; Martens, J.; Jacobs, P. A. *Appl. Catal.* **1987**, 31, 35.

(21) Fajula, F.; Ibarra, R.; Figueras, F.; Gueguen, C. *J. Catal.* **1984**, 89, 60.

(22) Argauer, R. J.; Landolt, G. R. U.S. Patent 1982.

(23) Arribas, J.; Corma, A.; Fornés, V. *J. Catal.* **1984**, 88, 374.

(16) Scaiano, J. C. *J. Photochem.* **1973/74**, 2, 81.

(17) Cozens, F. L.; García, H.; Scaiano, J. C. *J. Am. Chem. Soc.* **1993**, 115, 11134.

(18) Corma, A.; García, H.; Iborra, S.; Martí, V.; Miranda, M. A.; Primo, J. *J. Am. Chem. Soc.* **1993**, 115, 2177.

Table 1. Main Physicochemical Parameters of the Zeolites Used in This Work

zeolite	Si/Al ratio	Na ₂ O content (%)	crystal size (μm)	BET surface area (m ² /g)	nature of acid sites	overall acidity estimation ^c
HY	9.2 ^a	<0.02	0.8	576	more Brønsted than Lewis	1
H β	13 ^a	<0.02 (template free)			more Lewis than Brønsted	2
HMor	10 ^b	<0.02		550	more Brønsted than Lewis	3
HZSM5	26.5 ^b	<0.02 (template free)	1–3	420	mainly Brønsted	4

^a From MAS NMR. ^b From chemical analysis. ^c Ranging in order of increasing acid strength.

Table 2. Characteristic Data of the Composites Prepared in This Work

composite	amount of ABP (mg/g)	approximate (%) acid site occupancy	water content (wt %)	diffuse reflectance spectrum (λ_{max} , nm)	emission spectrum (λ_{max} , nm)	transient spectrum (λ_{max} , nm)
ABP–HY100	40.5	15	15.2	252, 337, 438	420–520	510, 720
ABP–H β	40.0	16	12.5	252, 337, 447	420–520	330, 440, 530
ABP–HMor	31.5	11	9.1	251, 409	420–520	330, 440, 530
ABP–HZSM5	27.7	35	8.0	250, 413 222, 300, 390 ^a	410–520 440	530 500, 750 ^b
ABP				250–350, 450 ^c	430	530 ^d
ABPH ⁺						

^a Diffuse reflectance of solid crystals. ^b Transmission transient spectrum of an AcN solution. ^c Diffuse reflectance of a ABP–HCl solid sample. ^d Transmission transient spectrum of ABP in aqueous H₂SO₄ solution.

Inclusion Procedure. Activation of the acidic zeolite was accomplished prior to use by heating at 423 K under 10⁻¹ Torr of dynamic vacuum for 2 h. Then the solid was cooled to room temperature, and a solution of ABP (~100 mg/g of wet zeolite) in isoctane (50 mL) was added under vacuum. The resulting suspension was magnetically stirred at 363 K for 2 h. After this time, the yellow solid was collected and submitted to continuous solid–liquid extraction using micro-Soxhlet equipment and CH₂Cl₂ as the solvent for several days. The resulting composite was dried at room temperature in air and then outgassed under reduced pressure (1–5 Torr) for 1 h. The samples were stored in vials under normal laboratory conditions.

Determination of the amount of ABP adsorbed onto the zeolite was carried out by measuring the absorbance of the recovered organic solutions at 315 nm using a Shimadzu spectrophotometer and comparing these values with a calibration plot. The corresponding amounts of ABP adsorbed onto the zeolite are contained in Table 2. The same inclusion procedure starting with 93 mg of ABP and NaY (1.0 g) did not lead to any appreciable adsorption of ABP.

GC analyses were performed with a Hewlett-Packard 5890 spectrometer equipped a flame ionization detector and a 25 m capillary column of 5% cross-linked phenylmethylsilicone. GC-MS analyses were carried out using a Hewlett-Packard 5988 A spectrometer equipped with the same type of column as the GC. Simultaneous thermogravimetric analyses and differential scanning calorimetry of the composites were carried out using a Netzsch STA 409 EP analyzer under a stream of air with a heating rate of 10 K min⁻¹. ¹H-NMR were recorded with a 400 MHz Varian Unity spectrometer in CDCl₃ solutions using TMS as internal standard.

In a few exploratory experiments 1-methylnaphthalene (Aldrich, used as received) was deposited onto the solids by stirring a suspension of the aromatic compound (75 mg) in CH₂Cl₂ (35 mL) and the corresponding composites (1.0 g) without any pretreatment at 273 K under reduced pressure until the solvent was completely removed. The resulting solids were outgassed under 10⁻¹ Torr of dynamic vacuum for 1 h and stored within closed vials.

Laser Flash Photolysis Experiments. The experimental setup for time-resolved diffuse reflectance is similar to that previously described.²⁴ The third or fourth harmonic (355 nm, 266 nm; ≤ 10 ns pulses; ≤ 20 mJ/pulse) from a Surelite Nd: YAG laser was used for sample excitation. Laser excitation at 355 nm was employed for the composites containing 1-methylnaphthalene. Samples placed in 3 \times 7 mm² Suprasil quartz cells were purged with nitrogen for at least 30 min prior to photolysis. Alternatively the solids were outgassed at 10⁻¹

Torr at room temperature or at 331 K for 1 h and backfilled with nitrogen before photolysis. After each data point, the sample was shaken to maximize the exposure of a fresh surface to the laser beam. Laser flash photolysis of ABP in homogeneous solution (ACN or 20% aqueous H₂SO₄) were performed using a transmission system²⁵ and static cells.

1,3-Cyclohexadiene Dimerization. The corresponding composite (250 mg) was added to a solution of 1,3-cyclohexadiene (50 mg) in CH₂Cl₂, and the suspension submitted to external irradiation for 1 h using a 250 W medium-pressure mercury lamp equipped with a Pyrex well refrigerated at 283 K. After this time, the suspension was filtered and the solid submitted to exhaustive solid–liquid extraction using CH₂Cl₂ as the solvent. The organic solutions were combined and appropriately diluted to record the UV absorption spectra. The amount of unreacted 1,3-cyclohexadiene was determined by UV measuring the absorbance at 240 nm. Product distribution was determined by a combination of ¹H NMR and GC of the reaction mixtures.

Results

Preparation and Characterization of the Complexes. HY zeolite was prepared starting from commercial NaY by two consecutive NH₄⁺-to-Na⁺ exchange–calcination processes, using increasing concentrations of aqueous solutions of NH₄AcO. The acidic mordenite (HMor) was obtained by HCl dealumination of a commercial sample in the sodium form. H β and HZSM5 were synthesized following reported procedures, calcined to decompose the organic template, and subjected to two consecutive NH₄⁺ exchange–calcination cycles. Table 1 contains the main physicochemical parameters of these four zeolites.

The acidity of these samples was investigated by monitoring the IR spectrum of pyridine retained within the zeolites after vapor adsorption onto fully dehydrated solids and subsequent desorption at increasing temperatures. The intensity of the 1550 and 1450 cm⁻¹ bands of pyridine constitutes a quantitative estimation of the population of Brønsted and Lewis acid sites, respectively, while changes in the intensities with the desorption temperature reports on the acid strength distribution of the solids (Table 1). Figure 2 shows the results attained for the HMor and HZSM5 zeolites. Relevant to this work, and in good agreement with

(24) Wilkinson, F.; Kelly, G.; Diffuse Reflectance Flash Photolysis. In *Handbook of Organic Photochemistry*; Sciaiano, J. C., Ed.; CRC Press: Boca Raton, FL, 1989; Vol. 1, p 293.

(25) Hadel, L. M. Laser Flash Photolysis. In *Handbook of Organic Photochemistry*; Sciaiano, J. C., Ed.; CRC Press: Boca Raton, FL, 1989.

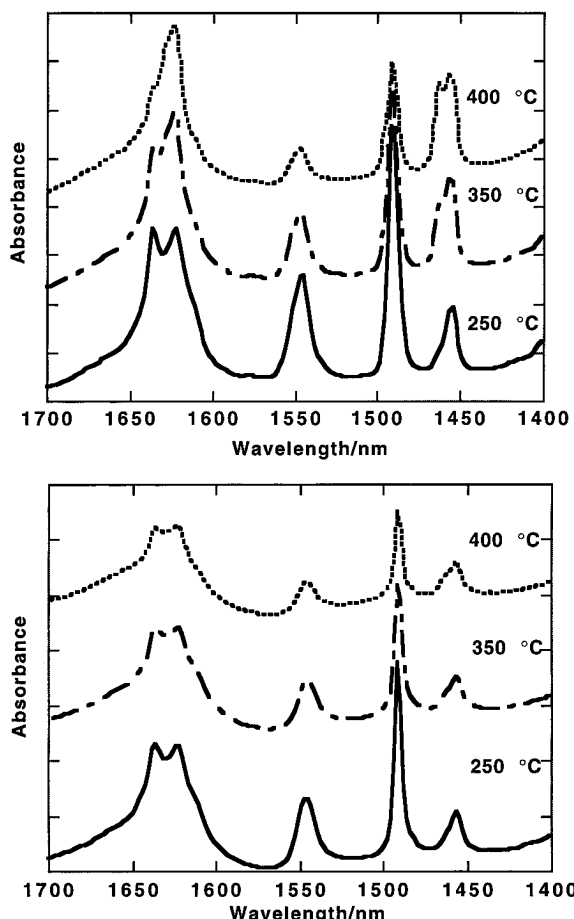


Figure 2. FT-IR spectra of the pyridine retained onto HMor (top) and ZSM5 (bottom) after adsorption from the vapor phase at room temperature and subsequent desorption by heating successively at increasing temperatures under 10^{-1} Pa for 1 h.

previous acidity measurements,^{26,27} was the lower acidity of the HY sample relative to the other zeolites.

Inclusion of the organic guest was carried out by stirring at 363 K for 2 h a suspension of ABP in isooctane with the corresponding acid zeolite previously activated by thermal treatment at 423 K under 10^{-1} Torr of dynamic vacuum for 2 h. The resulting solids were collected and submitted to continuous solid-liquid extraction for 4 days using CH_2Cl_2 as the solvent. The amount of ABP retained by each solid as well as the percentage of site occupancy are given in Table 2 and were calculated from the difference between the starting weight and the total ABP recovered in the combined organic solutions measured by UV spectrophotometry. Even though the organic solutions developed a slight light yellow color during the inclusion procedure only unchanged ABP was detected by GC-MS analyses after the solids were subjected to continuous solid-liquid extraction using CH_2Cl_2 as the solvent. The composites were finally outgassed to remove the solvent and stored without any special precautions. The same treatment using the nonacidic sodium form of the Y faujasite (NaY) led to an almost complete recovery (>90%) of the starting ABP.

Differences in the ground-state complexation of ABP in the four acidic hosts are evident from the diffuse

(26) Climent, M. J.; Corma, A.; Garcia, H.; Iborra, S.; Primo, J. *Stud. Surf. Sci. Catal.* **1991**, 59, 557.

(27) Farneth, W. E.; Gorte, R. J. *Chem. Rev.* **1995**, 95, 615.

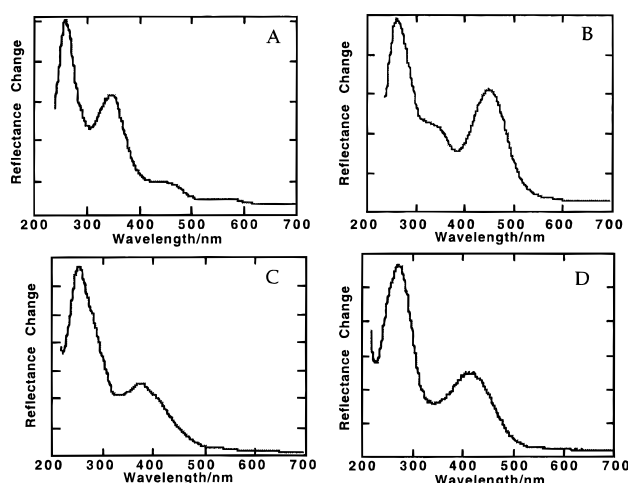


Figure 3. Diffuse reflectance spectra of (A) ABP-HY, (B) ABP-H β , (C) ABP-HMor, and (D) ABP-HZSM5.

reflectance spectra of the yellow solids (Figure 3). The characteristic λ_{max} obtained with the zeolite complexes and with solid ABP in its basic and acidic forms are given in Table 2.

The strength of the adsorption of ABP within the acid zeolites as well as the equilibrium content of coadsorbed water was studied using thermogravimetric analysis (TG) coupled with differential scanning calorimetry (DSC). The scan shows an initial loss of weight, corresponding to an endothermic process, that can be ascribed to the transition of adsorbed water to the vapor phase. The reduction of the weight up to 473 K due to the loss of water for each composite is included in Table 2. The data fit well with the known relationship between zeolite type and hydrophilicity.²⁸ On the other hand, the loss of weight corresponding to the exothermic region of the DSC (473–773 K) agrees reasonably well with the estimated amount of ABP retained onto the solids after solid-liquid extraction (Table 2). Except for the HY composite, no sharp minimum of the TG-DSC corresponding to the decomposition of the adsorbed organic material was observed. This implies that the ABP molecules do not interact with the same strength with the different acid sites, but rather adsorbed ABP is experiencing a wide distribution of acid strengths. Previous titration of HY by means of pK_a indicators established the population of the sites with different acid strength.²⁹

In the case of the more hydrophilic ABP-HY sample, additional analyses 60 days after sample preparation were performed. Exactly the same DSC profiles and values were obtained, which indicates that the water saturation value had already been reached within the first weeks after the sample preparation and that readsorption and relocation of regained water does not produce irreversible changes during the time period considered.

The interaction between the weakly basic ABP guest and the acid sites of the different zeolite hosts can be better examined by analyzing the FT-IR spectra of the composite materials. From the guest standpoint it is well-known³⁰ that the wavenumber of the C=O stretching band in aromatic ketones is very sensitive to

(28) van Bekkum, H.; Kouwenhove, H. W. *Recl. Trav. Chim. Pays-Bas* **1989**, 108, 283.

(29) Corma, A.; Garcia, H.; Primo, J. *J. Chem. Res. (S)* **1988**, 40.

substituent effects. In particular, isotopic labeling has established that complexation through the NH_2 group of ABP shifts this absorption from 1635 cm^{-1} to higher wavenumbers, with an absorption of 1652 cm^{-1} being reported for Lewis acid complexes of ABP with SnX_4 .³¹ On the other hand, it has been found³² that in solution the $\text{C}=\text{O}$ stretching frequency is very dependent on the nature of the medium such that increasing solvent polarity tends to lower the frequency. The maxima of the $\text{C}=\text{O}$ band for ABP included within acidic zeolites was recorded for each zeolite at about 1640 cm^{-1} . However, the broadness of the absorption together with the close similarity of the $\text{C}=\text{O}$ stretch for ABP and ABP-HCl does not allow a definite conclusion to be made about the protonation of the aromatic amino group. In addition, the presence of coadsorbed water, which exhibits a bending vibration in this region, also interferes in the assignment of $\text{C}=\text{O}$ vibration band. In the case of the ABP-HZSM5 sample, the IR spectrum showed a shoulder at 1678 cm^{-1} in addition to the 1640 cm^{-1} band that could be resolved into two new maxima at 1645 and 1635 cm^{-1} by outgassing the wafer at 473 K for 1 h under 10^{-1} Pa dynamic vacuum.

In the case of the less acidic HY solid, a series of spectra were recorded after thermal treatment of the wafer for 1 h under dynamic vacuum at increasing temperatures (100 , 200 , 300 , and $400\text{ }^\circ\text{C}$). It was anticipated that a progressive desorption of the more loosely retained ABP as well as evacuation of neutralizing water spectator molecules would produce significant changes in the IR spectrum. The FT-IR shows the disappearance of the characteristic carbonyl vibration band at 1640 cm^{-1} , and a concurrent increase in the adsorption in the 1500 – 1300 cm^{-1} region upon increasing the temperature to $400\text{ }^\circ\text{C}$. Such changes are expected for protonation of the $\text{C}=\text{O}$ group ($\text{p}K_a = 6.86$ ³³) and it has been reported that HY has a small population of acid sites with this acidity.³⁴

The interaction of the zeolite with ABP was also investigated from the host standpoint. Thus, inclusion of the base must produce some changes in the acidic OH groups observed in the 3700 – 3400 cm^{-1} zone of the IR spectrum. The very special monodirectional topology of HMor zeolite must impose severe restrictions on the diffusion of the guest through the internal voids compared with the open tridirectional Y and β geometries. Comparison of the FT-IR spectrum of the original HMor zeolite with the ABP-HMor complex reveals that a significant portion of the acidic OH groups located within the channels and characterized by the 3609 cm^{-1} band have disappeared, replaced by new absorption bands at 3505 , 3405 , and 3310 cm^{-1} assigned to the N–H bond stretching of the guest molecules. While the first two bands can be ascribed to aromatic amines, the last absorption is characteristic of the presence of ammonium cations,³⁰ in good agreement with the transient spectrum recorded for this sample (vide infra).

(30) Silverstein, R. M.; Bassler, G. C.; Morrill, T. C. *Spectroscopic Identification of Organic Compounds*, 4th ed.; John Wiley: New York, 1981.

(31) Vezzosi, I. M.; Zanoli, A. F.; Peyronel, G. *Spectrochim. Acta* **1980**, *36A*, 219.

(32) Weikwitsch, C. E. *Monatsh. Chem.* **1979**, *110*, 301.

(33) Mindl, J.; Vecera, M. *Coll. Czech. Chem. Commun.* **1970**, *35*, 950.

(34) Corma, A.; Garcia, H.; Primo, J.; Sastre, E. *Zeolites* **1991**, *11*, 593.

Analogous features were observed for the ABP-HZSM5 composite, where desorption of the organic guest at increasing temperatures under vacuum regenerates the internal acidic protons characteristic of the original HZSM5 zeolite.

Time-Resolved Diffuse Reflectance Laser Flash Photolysis of the Complexes. We have already shown that time-resolved diffuse reflectance is a convenient technique for the study of photochemical organic reactions within opaque media.³⁵ Photolysis of the composites was accomplished using the third or fourth harmonic (355 or 266 nm, respectively) from a Nd:YAG laser. The results obtained were independent of the excitation wavelength despite the fact that the protonated and unprotonated form of ABP have different absorption spectra.

The transient reflectance spectra recorded for the four different complexes are presented in Figure 4. The λ_{max} of the time-resolved reflectance spectra are summarized in Table 2 along with the λ_{max} of the transient absorptions spectra generated upon excitation of ABP in its acidic and basic forms in solution. From Figure 4 it is apparent that the structure and the physicochemical parameters of the zeolite greatly influences the transient spectra of the guest. The spectrum recorded for the ABP–HY composite shows two distinctive maxima and closely resembles that for ABP in homogeneous solution,³⁶ perhaps reflecting the loose environment. By contrast, the transient spectra obtained for the other two large-pore zeolites ABP–H β and ABP–HMor are similar with three resolved bands. The tight fit of the guest in the ZSM5 structure is again evident by a very distinctive spectrum of the ABP–HZSM5 composite, where only one maximum centered at 530 nm is present. Absorption at 530 nm is characteristic of triplet absorption of a large variety of substituted benzophenones.^{37,38}

To get experimental evidence for the assignment of these transients, the influence of the presence of oxygen was investigated. It has been established that in the case of highly hydrophilic zeolites, the presence of coadsorbed water strongly impedes oxygen diffusion through the micropores, reducing or even eliminating any quenching effect.³⁹ The presence of extraframework aluminum, responsible for the Lewis acidity of the zeolites (see Table 1 and Figure 2), can also contribute to impede oxygen diffusion. Therefore, we treated the samples under vacuum at room temperature (ABP–HZSM5) or at 331 K (ABP–HY and ABP–HMor) for 1 h , before introducing oxygen to the samples. The transient spectra recorded under these conditions for ABP–HMor and ABP–HZSM5 are presented in Figure 5. While outgassing followed by the addition of O_2 was enough to establish the scavenging of the transient for the HZSM5 composite, no such effects could be observed for the most hydrophilic HY zeolite even after heating at 331 K . ABP–HMor represents an intermediate

(35) Bohne, C.; Redmond, R. W.; Scaiano, J. C. Use of the Photophysical Techniques in the Study of Organized Assemblies. In *Photochemistry in Organized and Constrained Media*; Ramamurthy, V., Ed.; VCH: New York, 1991; p 79.

(36) Godfrey, T. S.; Hilpern, J. W.; Porter, G. *Chem. Phys. Lett.* **1967**, *1*, 490.

(37) Carmichael, I.; Hug, G. L. *J. Phys. Chem. Ref. Data* **1986**, *15*, 1.

(38) Carmichael, I.; Hug, G. L. Spectroscopic and Intramolecular Photophysics of Triplet States. In *Handbook of Organic Photochemistry*; Scaiano, J. C., Ed.; CRC: Boca Raton, FL, 1989; Vol. I, p 369.

(39) Thomas, J. K. *Chem. Rev.* **1993**, *93*, 301.

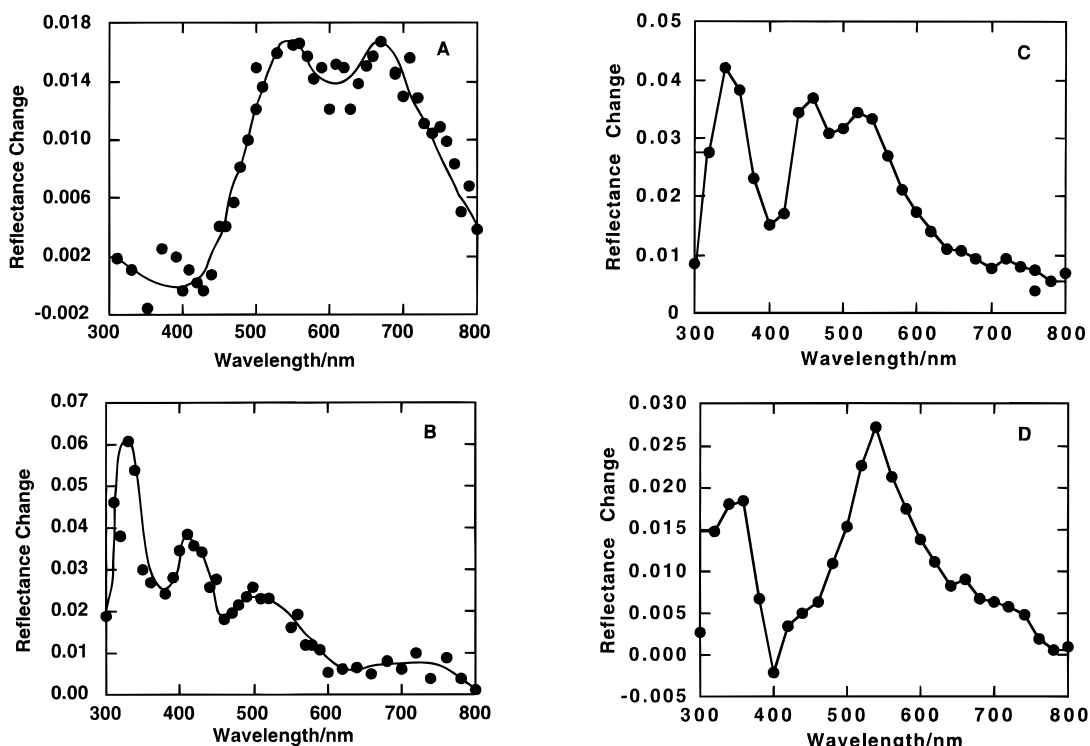


Figure 4. Transient diffuse reflectance spectra of (A) ABP–HY, (B) ABP–H β , (C) ABP–HMor, and (D) ABP–HZSM5 recorded 0.6 μ s after 266 nm excitation.

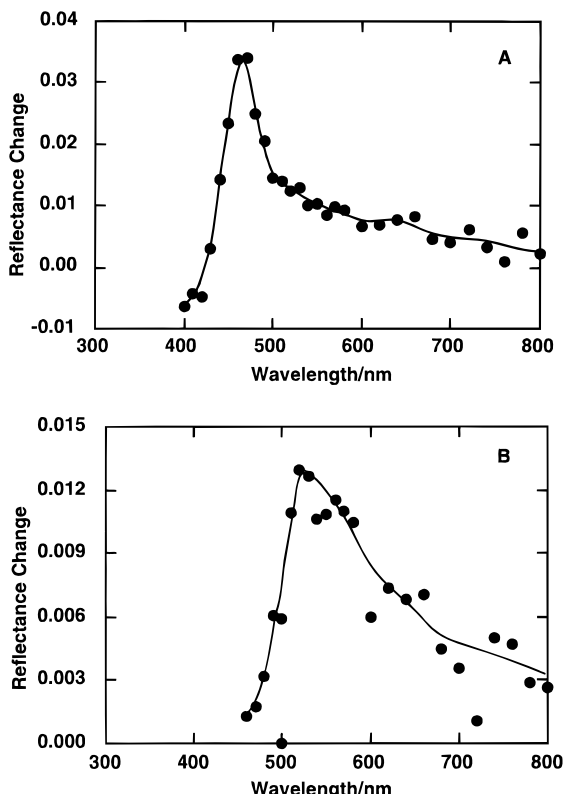


Figure 5. Transient spectra of (A) ABP–HMor and (B) ABP–HZSM5 recorded under the same conditions as those in Figure 4 after outgassing for 1 h at (A) 331 K or (B) room temperature before opening to the air.

situation. As characterization of the composites has revealed that thermal treatment alters the properties of the guest no attempts were made to evacuate the coadsorbed water at higher temperatures. It is noteworthy that the conditions required to observe oxygen quenching depends on the water content of the compos-

ite (Table 2). Finally, the transient spectra of ABP–HMor and ABP–HZSM5 presented in Figure 5 regained the characteristics of those in Figure 4 after several days, showing that the changes are not due to irreversible modification of the guest. It should be noted that purging a solution of ABP with O₂ for 5 min was sufficient to completely quench the transients in the time domain we can monitor.

1-Methylnaphthalene Quenching Experiments. The ability of the zeolite framework to influence the interaction between included ABP and a quencher was the subject of exploratory work using laser flash photolysis of composites containing 1-methylnaphthalene (MN). MN was added to the sample by stirring at 273 K a suspension of MN and untreated ABP–HY composite in CH₂Cl₂ under reduced pressure, until the solvent was completely removed. Since quenching in solid samples under dry conditions is complicated by the severe mobility restriction imposed on the photosensitizer and the quencher, a high molar ratio of MN:ABP (corresponding to 1 molecule of MN/ α -cage of HY zeolite) was used. The same amount of MN was added to the other composites, following exactly identical protocol.

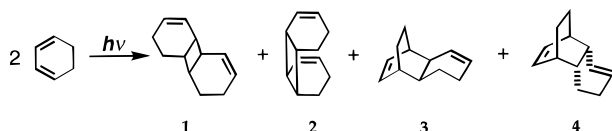
The presence of such a large amount of MN was apparent in the emission properties of the solids recorded after excitation at 300 nm. Thus, instead of the usual fluorescence of naphthalene derivatives within ion-exchanged faujasites at 340 nm,⁴⁰ the appearance of an intense band around 400 nm attributable to the emission of MN excimers^{41,42} was observed. In the case of the large-pore zeolites, this band encompasses the region of the ABP phosphorescence, making it indistin-

(40) Ramamurthy, V.; Caspar, J. V.; Eaton, D. F.; Kuo, E. W.; Corbin, D. R. *J. Am. Chem. Soc.* **1992**, *114*, 3882.

(41) Lim, E. C. *Acc. Chem. Res.* **1987**, *20*, 8.

(42) Tung, C.-H.; Wang, Y.-M. *J. Chem. Soc., Chem. Commun.* **1989**, 1891.

Scheme 2. Dimers Formed in the Photosensitized Irradiation of 1,3-Cyclohexadiene



guishable. The distinctive properties of the ABP–HZSM5 composite were again remarkable: only in this case the emission spectra showed resolved bands for ABP phosphorescence and MN excimers.

Photolysis of these composites was carried out at 355 nm excitation where MN has no absorption in solution. Control experiments showed that no transients arise from direct absorption of light by MN within NaY under our experimental conditions. In the case of the ABP–HZSM5 composite the transient spectrum due to ABP remains almost unaltered by the presence of MN suggesting that energy transfer is inefficient in this zeolite.

For the HY and HMor zeolites the transient spectra was complex and not readily interpretable. The common feature was a structureless absorption band from 400 to 650 nm that may be due to the T–T absorption of the MN excimers.⁴¹ In addition, the possibility that $MN^{\cdot+}$ radical cation with a characteristic absorption around 700 nm, could be formed in some extent cannot be completely ruled out.⁴³ As shown below, preparative experiments with 1,3-cyclohexadiene were far more informative.

1,3-Cyclohexadiene-Photosensitized Dimerization. From the preparative point of view, the application of these composite materials as photosensitizers under heterogeneous conditions was tested by performing the photodimerization of 1,3-cyclohexadiene. This photocycloaddition can also be used as a model reaction to determine the ability of these composites to behave as energy or electron-transfer sensitizer under wet conditions. Previous studies have established that the ratio between the regio- and stereoisomers **1–4** (Scheme 2) is strongly dependent on the reaction mechanism. Thus, energy transfer leads to predominant formation of the [2+2] dimers, while the single electron transfer (SET) mechanism leads to the [4+2] dimer **3** as the major product.⁴⁴

The possibility that dimerization could be due to the adventitious interaction with the zeolite framework without participation of the guest has to be addressed, since it has been found that the thermal and photochemical dimerization of 1,3-cyclohexadiene adsorbed within NaX faujasite gives a mixture of **3:4** (1:3.8) through a SET mechanism.⁴⁵

Photolysis was carried out using a 125 W medium-pressure mercury lamp by stirring at room temperature a suspension of the corresponding composite and 1,3-cyclohexadiene in CH_2Cl_2 through a Pyrex filter. Oxygen removal was crucial in order to avoid the formation of appreciable amounts of undesired oxidation products. A series of control experiments, including the photolysis of 1,3-cyclohexadiene in CH_2Cl_2 , the homogeneous irradiation of 1,3-cyclohexadiene in CH_2Cl_2 containing

ABP or 2,4,6-triphenylpyrilium tetrafluoroborate (TPT)⁴⁶ and the heterogeneous irradiation of 1,3-cyclohexadiene in CH_2Cl_2 in the presence of NaY⁴⁷ were carried out simultaneously under exactly the same experimental conditions. After photolysis, the zeolite composites were submitted to continuous solid–liquid extraction using CH_2Cl_2 as the solvent in order to increase the mass balance and to minimize inaccuracies in the product distribution due to differences in the internal diffusion of the dimers. The results attained are given in Table 3.

The lack of formation of any product in the direct photolysis of 1,3-cyclohexadiene or in the presence of NaY clearly established that dimerization in the zeolite composites under our experimental conditions is due to the guest acting as a photosensitizer. Moreover, while the product distribution for the TPT photosensitization is consistent with SET 1,3-cyclohexadiene dimerization, matching the values reported in the literature,⁴⁸ the results for homogeneous ABP photodimerization are very similar to those previously found using unsubstituted benzophenone⁴⁹ and are representative of the energy transfer photodimerization.

It is worth noting that the dimer ratio using the different zeolite-hosted ABP were very similar and closely resemble that of the energy-transfer mechanism. A remarkable difference was the mass balance after the photochemical reaction, probably reflecting differences in the 1,3-cyclohexadiene adsorption or thermal decomposition and polymerization within the acidic framework.

Discussion

Location of the ABP in the Different Environments. Inclusion of ABP within the zeolites was carried out by allowing free diffusion of the guest from a nonpolar solution to the thermally activated zeolite. Due to the high hydrophilicity and water content of zeolites, prior evacuation was found to be necessary in order to adsorb the organic compound. In addition, specifically in the case of acidic zeolites, it is well established that their catalytic activity is significantly decreased by the presence of water.

Interaction of ABP with the zeolite framework must be sufficiently strong that considerable amounts of this guest are retained after exhaustive solid–liquid extraction. A comparison with the sodium form of the Y faujasite reveals that both the geometrical structure and the presence of acidic sites plays a significant role in this interaction. In fact, the strength of the interaction can be characterized by the thermogravimetric analysis profiles of these composites and the changes in the IR spectrum after successive treatment at increasing temperatures. From these data, it was established that ABP remains essentially unaltered below 473 K, while

(46) Miranda, M. A.; García, H. *Chem. Rev.* **1994**, *94*, 1063.

(47) It has been observed that 1,3-cyclohexadiene adsorbed onto some acid zeolites does undergo dimerization upon irradiation. However, the dimer distribution points to a SET mechanism similar to that reported in ref 45 and different to that observed here using ABP as photosensitizer. A full account will be reported elsewhere (Fornes, V.; García, H.; Miranda, M. A.; Mojarrah, F., unpublished results).

(48) Mattay, J.; Gersdorf, J.; Mertes, J. *J. Chem. Soc., Chem. Commun.* **1985**, 1088.

(49) Valentine, D.; Turro, N. J.; Hammond, G. S. *J. Am. Chem. Soc.* **1964**, *86*, 5202.

(43) Shida, T. *Electronic Absorption Spectra of Radical Ions*; Elsevier: Amsterdam, 1988; Vol. Physical Science Data 34.

(44) Müller, F.; Mattay, J. *Chem. Rev.* **1993**, *93*, 99.

(45) Ghosh, S.; Bauld, N. L. *J. Catal.* **1985**, *95*, 300.

Table 3. Results of the Photosensitized Dimerization of 1,3-Cyclohexadiene

sensitizer ^a	mass balance (%)	recovered by extraction (%)	unreacted CH (%)	yield of the dimers (%)	turnover no. (yield/mg of ABP)	ratio 1:2:3:4
ABP	<i>b</i>		0	85		2.5:1:1.5:0
ABP-HY	68	44	25	40	4.0	2.5:1:1.5:0
ABP-H β	83	21	10	70	7.0	2.5:1:1.5:0
ABP-HMor	92	26	25	65	8.0	2.5:1:1.5:0
ABP-HZSM5	92	6	75	15	2.1	4.5:1.5:2.5:1
TPT	<i>b</i>		<5	75		0.0:1.6

^a No reaction products were detected under the same conditions in the irradiation of a CH₂Cl₂ solution of 1,3-cyclohexadiene (4 \times 10⁻² M), even in the presence of NaY (250 mg). ^b The whole reaction mixture was analyzed.

the decomposition of the guest occurs at higher temperatures and is complete around 823 K. It is possible that in the intermediate region protonation of the carbonyl group can take place.

The distinctive ability of the zeolite microenvironment to influence the ground state of the guest is revealed by the shifts of the maxima in the diffuse reflectance spectra of the solids. Modification of the electronic spectra of ABP in homogeneous solution by solvent polarity⁵⁰ or protonation⁵¹ has already been established. Moreover, the band above 400 nm in the diffuse reflectance has been assigned to the interaction of the ABP NH₂ group with acid sites.³¹

These results strongly suggest that ABP is located within the internal voids of the solids and, therefore, experiences different crystalline environments. An exclusive external location of ABP could not reasonably account for the dramatic changes observed in the absorption properties of the guest.

To address more specifically the issue of the ABP location, we can take advantage of the acidic nature of our hosts, which exhibit in the IR characteristic OH stretching bands for external silanols and for the different structural types of internal acidic protons. Therefore, if a basic guest is accommodated on the internal surface close to the acidic sites, a decrease in the intensity of the corresponding stretching band should be observed as a result of the inclusion procedure. A decrease in this intensity is indeed observed for the ABP-HMor composite. It should be noted that the diffusion of a molecule through the internal voids of Mor during the adsorption step is much more restricted than for the other large pore zeolites, due to the monodirectional topology of the former compared with the tridirectional open structure of Y and β .

Inclusion of ABP within the ZSM5 zeolite deserves a special comment. While the size of ABP is smaller than the micropore dimensions of 12 oxygen-membered zeolites (such as Y, β , and mordenite), docking using a molecular modeling⁵² predicts that ABP cannot enter through the 10 oxygen rings of the ZSM5 micropores and that if ABP is incorporated within ZSM5 overlap between ABP and the pentasil framework must be considerable. This prediction agrees with previous reports of the failure to include significant amounts of the parent benzophenone in pentasil structures.⁵³ However, since our inclusion procedure was carried out at a relatively high temperature, estimations made without taking into account a much higher vibration amplitude

of the lattice should not apply. The fact that after our inclusion procedure we have been able to detect spectroscopically by IR and ¹³C MAS NMR isoctane, a solvent that has been reported cannot penetrate through the micropores of medium-pore-sized zeolites,^{54,55} adsorbed on ZSM5 lend experimental support to our hypothesis.

In fact, all the experimental evidence from the ABP-HZSM5 composite indicates that ABP must be predominantly located within the internal surface. The high amount of ABP retained on the solid, the special features of the diffuse reflectance spectrum, the disappearance in the IR of the band at 3610 cm⁻¹ corresponding to the internal acidic OH stretching of the host, the carbonyl region of the IR spectrum and the laser flash photolysis experiments are consistent with the above explanation. However, the dramatic effect of the zeolite framework is still in agreement with the prediction of a strong guest-host overlapping.

From the global inspection of all these data we can conclude that in the samples we have prepared ABP is located in three different reaction cavities; one of them loose corresponding to the ABP-HY composite, another tight in the case of the ABP-HZSM5, and the other intermediate corresponding to the ABP-H β and the ABP-HMor composites.

Characterization of the Transient Spectra of the Composites. Upon photolysis, a large variety of substituted benzophenones give rise to triplets that typically decay in the microsecond time domain. These species usually exhibit a characteristic T-T absorption band around 530 nm. It has been reported that the transient spectra of ABP in propylene³⁶ glycol consists of two bands centered at 466 and 638 nm, reflecting the special nature of the amino substituent.³⁶ We have recorded these maxima in acetonitrile at 500 and 750 nm, indicating that these bands are very sensitive to the polarity of the medium. Therefore, it seems reasonable to assume that the same precursor, unprotonated ABP, is responsible for the transient spectrum of the ABP-HY composite, where the same two bands albeit broader, can be observed.

It has been reported that in 20% acidic aqueous solution the amino group of ABP is protonated.⁵¹ This is in agreement with the pK_a value of the conjugate acid. It is noteworthy that the transient spectra recorded for the homogeneous acidic solution shows only one band in the region where the T-T absorption of benzophenone triplets is generally observed. The transient spectrum of the ABP-HZSM5 composite has only one

(50) Kawska, A.; Ston, M. Z. *Naturforsch.* **1979**, 34a, 708.

(51) Ireland, J. F.; Wyatt, P. A. H. *J. Chem. Soc., Faraday Trans. 1* **1973**, 69, 161.

(52) Docking using Biosym Insight II Molecular Modeling package running on a Silicon Graphics work station.

(53) Casal, H. L.; Scaino, J. C. *Can. J. Chem.* **1985**, 63, 1308.

(54) Turro, N. J.; Cheng, C.-C.; L., A.; Corbin, D. R. *J. Am. Chem. Soc.* **1987**, 109, 2449.

(55) Turro, N. J.; Lei, X.; Cheng, C.-C. *J. Am. Chem. Soc.* **1985**, 107, 5824.

band centered at 530 nm accompanied by bleaching at 400 nm (Figure 4). Complete recovery of the ground-state absorption at 400 nm is observed as the 530 nm band decays. Moreover, the band at 530 nm is quenched by oxygen. Therefore, we assign this spectrum as the triplet state of protonated ABP.

An intermediate situation is observed in the case of ABP–H β and ABP–HMor, which again show a remarkable similarity. In addition to the 530 nm band, corresponding to the triplet of ABP H^+ and quenched by oxygen in the mordenite structure (Figure 5), other bands around 340 and 440 nm are present. The decays of these two bands over several time scales are different than the 530 nm band. The possibility that any of these bands could correspond to the ketyl radical arising from hydrogen abstraction from traces of isoctane from the inclusion step cannot be ruled out but seems unlikely in view of the reluctance of ABP to undergo hydrogen abstraction from amines in acetonitrile.⁵⁶

Energy Quenching within Zeolitic Media. MN and 1,3-cyclohexadiene were used as probes to learn about the influence of the zeolite microenvironment surrounding ABP on its properties as a photosensitizer. For the laser flash photolysis quenching experiments under dry conditions, MN was added to the composites by solvent removal from a suspension containing MN and the corresponding hydrated ABP–zeolite composites. This inclusion procedure has been found to be very inefficient for the incorporation of naphthalene molecules into the micropores of zeolites.⁴⁰ However, conditions under which the photosensitized molecule is located on the external surface are more likely to match those occurring when using these composites as heterogeneous photosensitizers.

Due to the different location of ABP and MN, the intimate contact during the photolysis seems unlikely. However, it has been found that sensitization only requires the presence of the quencher in the same or immediate neighboring cavity as the sensitizer.⁵⁷ We were interested in determining the ability of the zeolite framework to protect ABP from quenching.

The presence of MN alters the characteristic ABP spectra in the three large pore zeolites, while only minor changes in the spectrum of the ABP–ZSM5 composite were recorded. These results can be rationalized assuming that ABP is very well protected in the medium pore tight environment provided by the ZSM5 zeolite. A similar conclusion can be reached by comparing the turnover numbers obtained for the 1,3-cyclohexadiene dimerization (Table 3), which represents the percentage of dimer formed per mg of ABP included on the zeolite. The value for ABP–ZSM5 is much lower than that for the large-pore composites. This suggests that 1,3-cyclohexadiene is held at a distance near or beyond that required for reaction with excited ABP in that environment. This lack of interaction between ABP and MN

in the ABP–ZSM5 composite is also supported by the emission spectrum of the sample.

In the case of the 1,3-cyclohexadiene dimerization, energy-transfer processes to give predominantly [2+2] dimers **1** and **2** also prevail. However, formation of the *endo* [4+2] adduct **4**, absent in the homogeneous ABP photosensitization, was observed for the ABP–HZSM5 composite, indicating that a SET mechanism can also be operative to a minor extent.

Conclusions

ABP behaves in many ways as a typical energy-transfer photosensitizer in homogeneous solution,⁵⁸ giving rise to the formation of the MN triplet and [2+2] 1,3-cyclohexadiene dimers. Similar behavior has been observed in general for ABP incorporated within acid zeolites when the pore dimensions do not limit the approach severely. Experimental evidence has shown that this photosensitizer can be incorporated within the internal surfaces of large- and medium-pore zeolites. It has been found that the acidity of these solids plays an important role in the immobilization of hosted ABP.

The distinctive architecture of the confined space surrounding ABP determines the properties of its excited states and its ability as a photosensitizer. We have observed that the electrostatic fields of the internal zeolite surfaces tend to favor electron-transfer mechanisms compared with ABP in solution. In addition, the tight environment provided by the ZSM5 zeolite seems to protect ABP from interacting with the quenchers, while oxygen quenching is extremely dependent on the characteristics of composite and experimental conditions. Finally, ABP–H β and ABP–HMor have been found to be the most convenient heterogeneous photosensitizers of our series from a preparative point of view.

Although more information is necessary in order to predict the result of the photosensitization using these composite materials, our results point out how dramatically the properties of a photosensitizer can be modified by inclusion within zeolite microenvironments, and, therefore, the potential of zeolites as organized media to gain control and shape-selectivity on this type of photochemical reactions.

Acknowledgment. We thank the Natural Sciences and Engineering Council of Canada for an operating grant (J.C.S.) and the DGICYT of Spain (H.G., Grant PB93-0380) for financial support. H.G. thanks to the DGICYT for a fellowship and J.C.S. acknowledges the award of a Killam Fellowship from the Canada Council. Rosa Torrero is also acknowledged for her technical assistance recording FT-IR.

CM950311M

(56) Khan, J.; Cohen, S. G. *J. Org. Chem.* **1991**, *56*, 938.
(57) Scaiano, J. C.; Camara de Lucas, N.; Andraos, J.; García, H. *Chem. Phys. Lett.* **1995**, *233*, 5.

(58) Lissi, E. A.; Encinas, M. V.; Representative Kinetic Behavior of Selected Reaction Intermediates: Triplet States. In *Handbook of Organic Photochemistry*; Scaiano, J. C., Ed.; CRC Press: Boca Raton, FL, 1989; Vol. II, p 111.